ISSN: 0067-2904

Green Surfactant as a Soft Template for γ- Mesoporous Alumina Nanoparticles Preparation as Adsorbent and Carrier for Moxifloxacin Drug

Maryam A. Azeez , Sameer H. Kareem
Department of Chemistry-College of Science for Women-University of Baghdad, Iraq

Received: 19/4/2025 Accepted: 31/8/2025 Published: 30/10/2026

Abstract

The unique properties of nanomaterials, coupled with significant progress in nanotechnology, have driven a growing need for their manufacture. Additionally, because manufacturing processes generally result in increased pollution and environmental damage, there is a growing trend toward natural sources. In this study, a safe, environmentally friendly, and inexpensive natural surfactant was used as a soft template to synthesize mesoporous γ-alumina nanoparticles (γ-MNP). The template was the extracted solution of leaves of Zyziphus spina Christi, a widely available local plant, and aluminum nitrate as a precursor. The prepared γ-MNP was characterizing by using different analysis methods: FTIR, XRD, SAXRD, SEM, EDX, and AFM. Surface area was measured by the BET method, and porosity was measured by BJH. The prepared nanomaterials had a surface area (279.31 m^2g^{-1}), pore volume (0.572 cm^3g^{-1}) and pore diameter of 8.199 nm. The obtained BJH pore size distribution and average pore diameter and the hysteresis loops of the isotherms confirmed the mesoporous nature of the prepared sample. The XRD analysis shows that the sample is in a crystalline form with γ- phase and the SEM investigation shows that the sample appears to have nano-sized, smooth spherical, and high and regular agglomeration. The AFM histogram of granularity accumulation distribution shows that the particles range from 10 to 100 nm in composition (72%). The effectiveness of the manufactured γ-MNP as an adsorbent and carrier for moxifloxacin was tested.

Keywords: Mesoporous materials, γ-alumina nanoparticles, Green Surfactant, sol-gel, Moxifloxacin Drug.

أستخدام مادة فعالة سطحيا صديقة للبيئة كقالب ناعم لتحضير جسيمات نانوية من γ– ألومينا متوسطة المسام وتوصيفها وتطبيقها كحامل لدواء موكسيفلوكساسين

مريم عزيز ، سمير حكيم كريم
قسم علوم الكيمياء, كلية العلوم للبنات, جامعة بغداد, بغداد, العراق

*Email: sameerhk_chem@csw.uobaghdad.edu.iq

Open Access Articles. This articles is licensed under

الخلاصة

لقد أدت الخصائص الفريدة للمواد النانوية إلى جانب التقدم الكبير في تكنولوجيا النانو إلى زيادة الحاجة إلى تصنيعها. بالإضافة إلى ان عمليات التصنيع تؤدي عمومًا إلى زيادة التلوث والضرر البيئي، لذلك فان هناك اتجاه متزايد نحو المصادر الطبيعية. في هذا البحث، تم استخدام مادة فعالة سطحيا طبيعية آمنة وصديقة للبيئة وغير مكلفة كقالب ناعم لتخليق جسيمات نانوية متوسطة المسام من γ–ألومينا (γ–MNP). كان القالب عبارة عن محلول مستخلص من أوراق النباتات المحلية المتوفرة على نطاق واسع Zyziphus Spina Christi، ونترات الألومنيوم كمادة أولية. تم توصيف γ–MNP المحضر باستخدام طرق تحليل مختلفة: FTIR و XRD و SAXRD و SEM و EDX و AFM، وقياس مساحة السطح بطريقة BET والمسامية بطريقة BJH. أعطت المواد النانوية المحضرة مساحة سطح (279.31 م2 غم −1) وحجم مسام (0.572 سم3 غم −1) وقطر مسام (8.199 نانومتر). أكد توزيع حجم مسام BJH ومتوسط قطر المسام، ومنحني الرجوعية (hysteresis loops) في الايزوثيرم الطبيعة المسامية المتوسطة للعينة المُحضرة. يُظهر تحليل حيود الأشعة السينية (XRD) أن العينة في شكل بلوري ذي طور γ–، بينما أظهر فحص المجهر الإلكتروني الماسح (SEM) أن العينة تبدو نانوية الحجم، كروية ناعمة، وذات تكتل عالي ومنتظم. يُظهر الرسم البياني لتوزيع تراكم الحبيبات في المجهر الإلكتروني الذري (AFM) أن الجسيمات تتراوح بين 10 و100 نانومتر، بنسبة (72%). تم اختبار فعالية γ–MNP المُصنّع كمادة مازة وحاملة لدواء موكسيفلوكساسين.

1. Introduction

Mesoporous alumina (MA) is a chemical compound with the formula Al_2O_3, and its pore diameter can be in 2-50 nm range according to the IUPAC classification. Mesoporous alumina has been used in different applications because of its high specific area, large pore volume, controlled porosity, chemical inertness, and exceptional stability [1]. Mesoporous alumina is used in many applications as catalysts, catalyst supports, adsorbents, membranes, ceramics, and heat-insulating materials due to its unique physicochemical properties [2]. In field of biomedicine, γ-mesoporous Al_2O_3 is a great host for broad drug loading and regulated release (drug delivery) due to its chemical inertness and adjustable surface chemistry [3,4].

The synthesis of mesoporous alumina (MA) has been described using a number of methods, including ball milling [5], laser ablation [6], sol-gel [7], pyrolysis [8], hydrothermal methods [9], microemulsion [10], hard template [11], and soft template [12]. In the template synthesis method, the template is the primary setup for managing, influencing, and changing the morphology and dimensions of the material. The template method is easy to use, very predictable, and reproducible, and it successfully regulates the pore size, shape, and structure of the material [13]. The template, such as polymers [14], biological macromolecules [15], and surfactants [16], is formed during the reaction. Micelles of the template produce the desired product, and the internal polymerization of the molecules creates a certain spatial structure. In comparison to a hard template, a soft template is easier to remove, the experimental condition is mild and simple, the construction is simple, and it can synthesize different materials with various morphologies. Therefore, the template method is a current trend in the preparation of materials [17].

In recent years, surfactants have been found to significantly improve the properties of alumina when added to the preparation process. The selection of cationic, anionic, nonionic, and amphoteric surfactants is a key factor. Furthermore, the structure and nature of surfactants greatly affect the final mesostructures, pore sizes, and surface areas of mesoporous materials [18-21]. Conversely, chemical surfactants involve the use of poisonous compounds, energy, heat, and extremely high pressure. Furthermore, the byproducts are toxic, further damaging the ecosystem. Interest in the environmentally friendly synthesis of

Al_2O_3 NPs using plant extracts has increased recently due to the non-toxic, reasonably priced, and environmentally beneficial nature of plant sources [22, 23].

Zizyphus spina Christi (ZSC), a tree found in southern and central Iraq as well as various Middle Eastern countries, is one of the many native plant species that have not yet been used. The concentration of natural surfactants and saponins in ZSC is high and is present in more than 500 plant species. The saponin molecule includes hydrophobic and hydrophilic parts. The hydrophobic part is composed of a triterpenoid or steroid backbone, and the hydrophilic part consists of several saccharide residues [24]. Ahmadi and S. R. Shadizadeh [25] extracted four saponin glycosides from ZSC leaves. For more information on using ZSC as a natural surfactant, as reported in [26].

The aim of this research is to use the ZSC leaf extract as a natural surfactant soft template to prepare mesoporous γ-alumina nanoparticles (γ-MNP) powder using the sol-gel method. The prepared γ-MNP was characterized using FTIR, XRD, SAXRD, SEM, EDX, AFM, and N_2 adsorption – desorption techniques, offering a new foundation for creating adsorbent materials with superior adsorption capabilities as well as a moxifloxacin drug carrier.

2. Materials and methods used

2.1. Materials

Aluminum nitrate nonahydrate $Al(NO_3)_3 \cdot 9H_2O$ (Molar mass 375.134 $g.mol^{-1}$)and NaOH were obtained from BDH Chemicals Ltd., Poole, England. Moxifloxacine drug with empirical formula $C_{21}H_{24}FN_3O_4$ with molar mass 401.4 $g.\ mol^{-1}$, Purity≥98% obtained from Vintek Pharmaceuticals.

2.2. Preparation of the samples

From local farms in Baghdad, Iraq, 100g of fresh Zyziphus Spina Christi leaves were cut, cleaned with tap water and deionized water, and left at room temperature until dried. The dried leaves were ground into a powder and then heated in a beaker to 70 °C for 24 h in 1000 mL of distilled water. The solution was cooled to room temperature and then filtered using Whatman paper. The supernatant was used as a template. γ-MNP was prepared using the procedure described in [27] with minor modifications as follows: 100 mL solution of plant extract (solution A) and 18.75 g $Al(NO_3)_3.9H_2O$ was dissolved in 100 mL of distilled water (solution B). Subsequently, solution B was added dropwise to solution A while stirring for 30 min at 70 °C. The pH of the solution was then adjusted to 9 by adding sodium hydroxide (1M) incrementally and agitated to create white suspensions for approximately 120 min at 70 °C. The solution was then aged at room temperature for 20 h to complete conversion into a gel. The products were filtered, rinsed repeatedly with distilled water, dried in an oven set at 80 °C for 8 h, and then calcined in a 600°C muffle furnace for 4 h.

2.3. Adsorption procedure

Adsorption experiments were carried out by the batch method using 0.3 g of γ-MNP and 100 mL of drug solution (6 mg/L) in a 250 mL conical flask immersed in a thermostatic shaker bath and shaken at 298 K. At the end of the adsorption interval, the supernatant was centrifuged, and the concentration of the drug solution before and after the adsorption was determined using a UV-Vis Spectrophotometer (SHIMADZU) at a maximum wavelength (λ_{max}) of 293 nm. The removal efficiency (R%) of the system was calculated according to Equation 1

$$R\% = [\ (C_0 - C_t\ )/C_0\ ] \times 100 \quad \ldots\ldots (1)$$

Where C_o is the initial concentration (mg/L), C_t is the concentration (mg/L) at any time.

2.4. Characterization

2.4.1. FTIR

FTIR, Prestige-21Fourier Transform, (Shimadzu Corporation, Japan), was used to characterize the prepared materials. The characteristic absorption bands were recorded in the range 4000 to 400 cm^{-1} were recorded.

2.4.2. XRD

XRD and SAXRD, Siemens, Cu Kα (λ =1 .541Å), were employed to confirm the microporosity and identify the phase type and crystallinity of the produced alumina, respectively, and the evaluation of the diffractograms took place between 2Θ = 10–80° for XRD and between 2Θ = 0–10° for SAXRD.

2.4.3. Porosity

The BET surface area and BJH porosity were calculated using Autosorb-1 software (Quantachrome Instruments). Prior to the test, 0.0849 g of the sample was degassed under vacuum at 120°C for 2 h.

2.4.4. Scanning Electron Microscope (SEM) and Energy Dispersive X-Ray (EDX)

SEM and EDX (Thermo Fisher Scientific Inc) were used to characterize the structure and morphology of the adsorbents at an accelerating scan voltage of 5.00 kV.

2.4.5 Atomic force microscopy (AFM)

AFM (Nanosurf, Shanghai, China) was used to obtain the topography and particle size distribution.

3. Results and Discussion

3.1. Fourier-transform infrared spectroscopy (FTIR):

FT-IR spectrum of the prepared γ-MNP was illustrated in figure 1. The peak at 1630 cm^{-1} is attributed to the bending vibration of the hydrogen-bonded surface hydroxyl groups of the physically adsorbed water molecules, whereas bands around 1385.04 cm^{-1} are associated with Al–O–H symmetric bending. The broad band in the region of 3452 cm^{-1} is caused by the Al–OH stretching vibration [28]. The peak at 1105 cm^{-1} relates to asymmetric bending of Al–O–H of the chemically adsorbed water on the alumina surface. The stretching vibrations of the distinctive bands of the Al–O and Al–O–Al bonds of γ alumina are shown by a broad and strong peak that appears in the 785 cm^{-1} to 624 cm^{-1} range [29, 30]. The small peak at 2951 cm^{-1} corresponds to the stretching (Al) O–H vibrations of AlOOH in boehmite [31]. These functional groups confirm the potential of this surface as an excellent adsorbent.

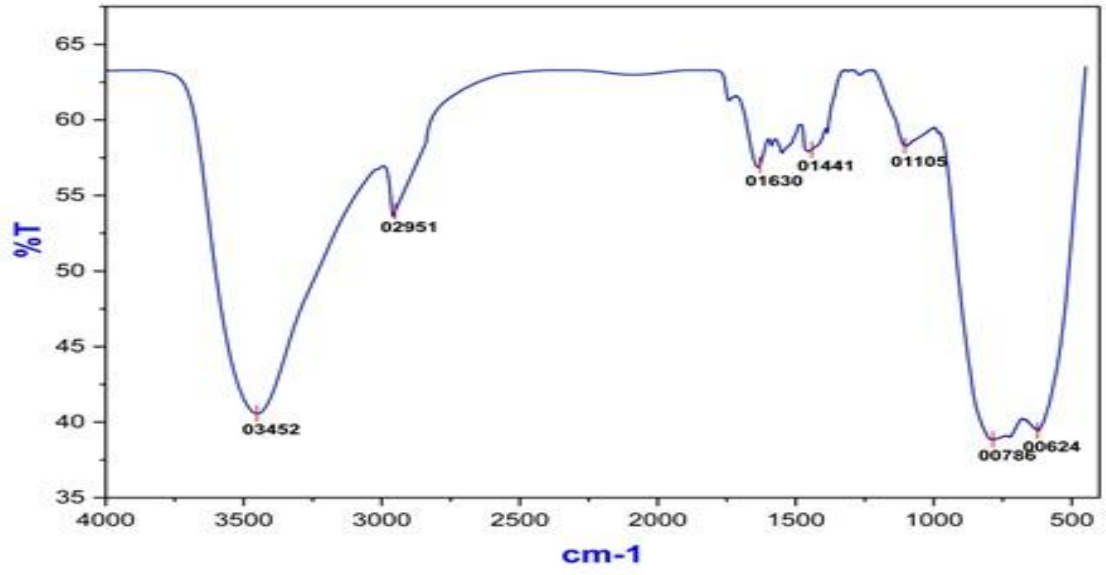

Figure 1: FTIR spectrum of γ-MNP after calcination

3.2. X-ray diffraction (XRD) and small-angle XRD (SAXRD):

Through X-ray diffraction analysis, the produced γ-MNP's crystallinity was ascertained; the findings are shown in Figure 2a and the data of the two highest peaks are listed in Table 1. The diffraction patterns of γ-MNP as determined by the intense peaks observed at 2θ= 19.431°, 37.707°, 45.875°, 60.832°, and 66.893°, correspond to the lattice planes (1 1 1), (1 3 1), (0 4 0), (3 3 3), and (0 4 4) and corresponding spacing values of 4.56453, 2.38375, 1.97650, 1.52151 and 1.39760 Å respectively. The observed relative intensities and lattice parameters of the diffraction peaks closely match the database of the Joint Committee on Powder Diffraction Standards (JCPDS) card file 96-154-1583. Thus, explaining the crystalline and exhibit cubic crystal structure represented by empirical formula of Al10.66O16.00 with space group Fd-3m. Similar diffraction pattern has been observed for γ-alumina by Krokidis et al [32], and reported of Al2O3-nanoparticles prepared using green methods [33].

The low-angle XRD patterns [Fig. 2(b)] showed no peak, indicating that the samples had mesopores with not only low regularity in size but also a broad size distribution.
Using Debye- Schere's equation, the crystal size was determined using equation 1 [34]:

$$D = K\lambda/\beta\cos\theta \quad (1)$$

Where D= size of the crystal (nm) K= Scherer constant (0.9), i x-ray source wavelength (0.15406 nm), β = FWHM (radians), and θ = peak position (radians). The crystallite size obtained using the peak of the lattice plane (044) was 3.27 nm, and that obtained using the peak lattice plane (040) was 4.06; thus, the average crystallite size was 3.67.

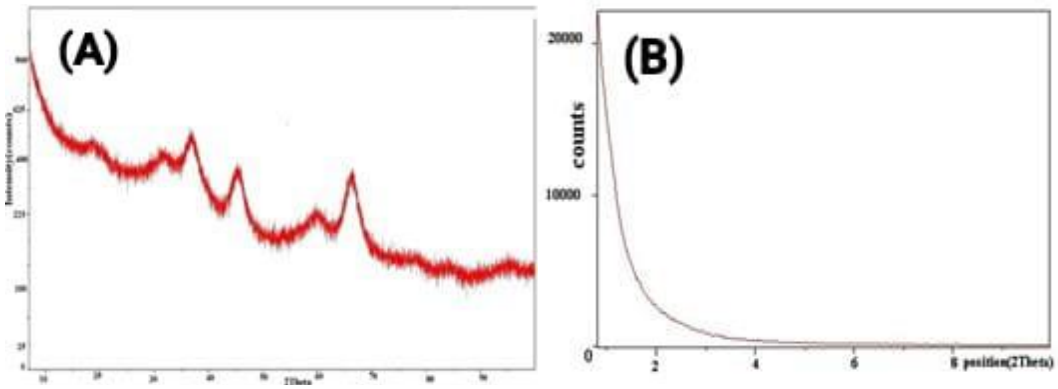

Figure 2: A: XRD patterns and B: SAXRD patterns of γ-MNP

Table 1: Lattice parameters of the prepared γ-MNP for the two highest peaks

Pos.(2 θ°)	h	k	l	d[Å]	FWHM (2 θ°)	I i]
45.875	0	4	0	1.97650	2.2191	65.7
66.893	0	4	4	1.39760	2.7368	100.0

3.3. Porosity:

The prepared γ-MNP was also examined using Nitrogen adsorption-desorption isotherm at 77 K to determine its surface area using the Brunauer–Emmet–Teller (BET) method and its porous texture using the Barret–Joyner–Halenda (BJH) method. The pore volume was calculated using the nitrogen adsorption volume at a relative pressure (P/Po) of 0.99. All results were illustrated for isotherm and the corresponding pore size distribution in Figure 3 and tabulated in Table (1) below.
Figure 3a shows that according to the IUPAC classification, the synthesized sample has pores in the mesoporous region (diameter 2-50 nm) with type IV isotherm [35]. The BET specific

surface area and pore volume obtained were (279.31 m2.g-1) and (0.5725 cm3.g-1) respectively, while the BJH estimations for the pore size distribution based on adsorption information showed a wide distribution for the sample with an average pore diameter of 8.1991 nm. The isotherms also showed a H2(a) hysteresis loop, indicating that the prepared sample has an ink bottle type [1, 36]. For comparison, an eco-friendly approach for synthesizing mesoporous alumina produced 340.15 m2.g-1[19], and sol-gel synthesizing produced porous γ-Al2O3 with specific surface area, 261.22 $m^2.g^{-1}$[4].

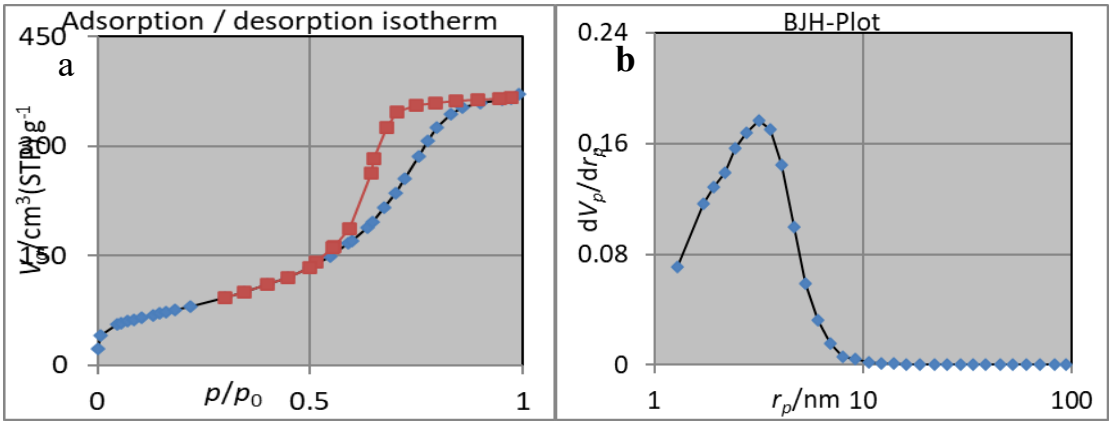

Figure 3: (a) N_2 adsorption/desorption isotherms and (b) -MNP pore-size distributions of γ-MNP

Table 1: Summary report of porosity Analysis and Surface Area for γ-MNP

parameter	S/ m-Al_2O_3
Surface area, BET	279.31 [m^2 g^{-1}]
Total pore volume (p/p^0=0.990)	0.5725 [cm^3 g^{-1}]
Average pore diameter	8.1991 [nm]

3.4. Scanning Electron Microscopy (SEM) and Energy Dispersive X-ray (EDX):

The morphology of the powder was examined by SEM, as shown in Figure 4. The micrograph reveals that the prepared γ-MNP particles appear to have nano-sized, smooth spherical, and high and regular agglomeration. However, no information was provided regarding the possession of permeable buildings. The particle sizes range from 43.78 to 50.53 nm and are approximately uniform and essentially homogeneous.

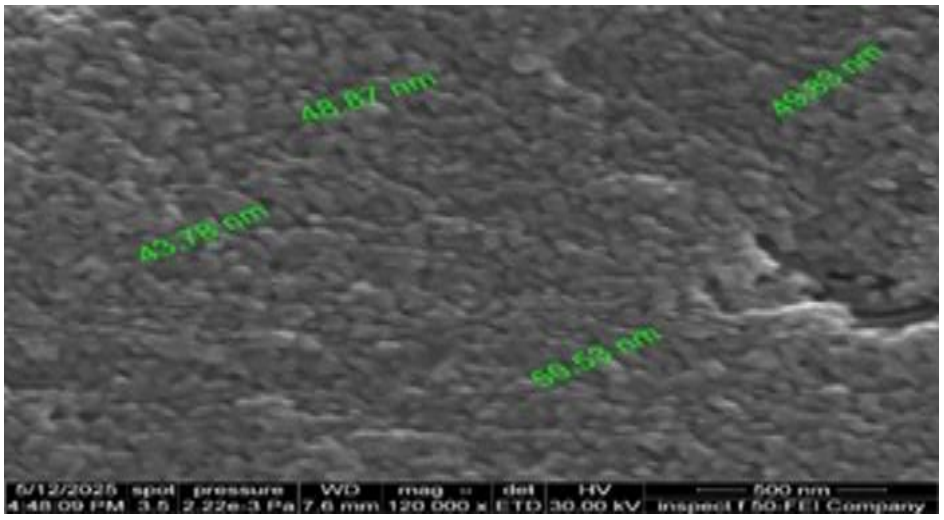

Figure 4: SEM image of the prepared γ-MNP

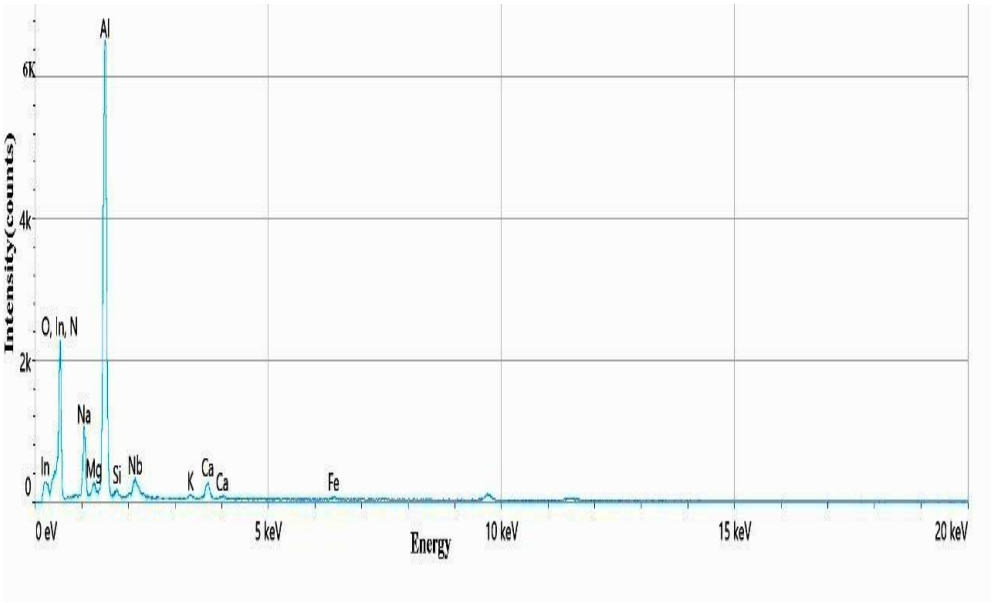

Figure 5: EDX spectrum of the prepared γ-MNP

The chemical composition of the generated powder was identified using EDX analysis, as shown in Figure 5 and Table 2. The percentage of aluminum oxide was very high, equal to 93 % by weight, and the EDX spectroscopy measurements confirmed the presence of carbon-free alumina.

Table 2: EDX results for γ-MNP Powder

Element	Atomic %	Atomic error percentage	Weight %	Weight % error
O	54.4	0.6	45.1	0.5
Al	41.0	0.1	47.9	0.2
Na	2.1	0.1	3.1	0.1
Mg	0.8	0.1	1.0	0.1
Ca	0.9	0.0	1.8	0.0
Si	0.8	0.1	1.1	0.1

3.5. Atomic force microscopy (AFM)

The topography of the synthesized γ-MNP was determined using AFM. Figure 5 shows the AFM images of the sample in two and three –dimensional in addition to the histogram of their particle size distributions.

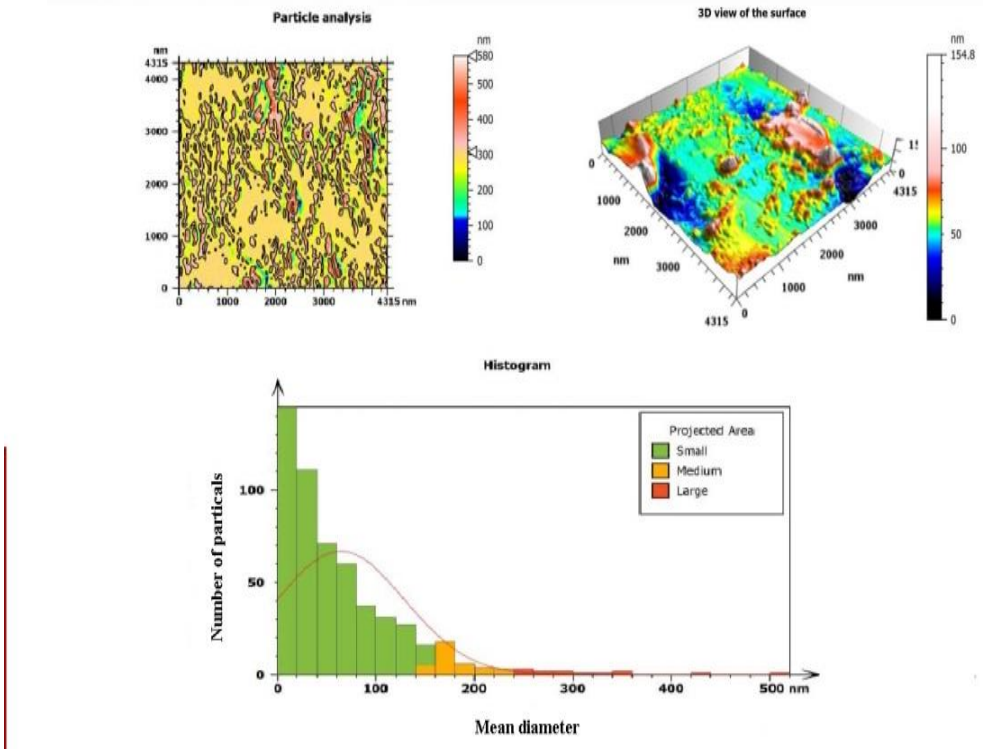

Figure 5: Histogram and distribution of granules and two- and three-dimensional view image for γ-MNP

Figure 5 demonstrates that the prepared γ-MNP sample has small spherical particles aggregating in spherical agglomerates. The results of the figure also showed that the particle size distribution was in the range (10-500 nm), and the particles ranged from 10 to 100 nm, as shown in the histogram of granularity accumulation distribution, comprising 72% of the total particles, while the other range from 100 -500 nm of the particle size composed 28% of the total particles. In addition, the images show a high degree of arrangement in the surface objects of the sample.

The prepared γ-MNP used as an adsorbent to remove the moxifloxacin (MOX) drug from the aqueous solution. From the results illustrated in Figure 6, approximately 47.64% of MOX was removed when the initial concentration was 6 mi L^{-1}. This removal efficiency was consistent with the results of previous studies [36, 37]. Nevertheless, it is not possible to eliminate the entire drug. This could be the result of many variables that affected the adsorption process, such as temperature, solution pH, and adsorbent dosage. [38].

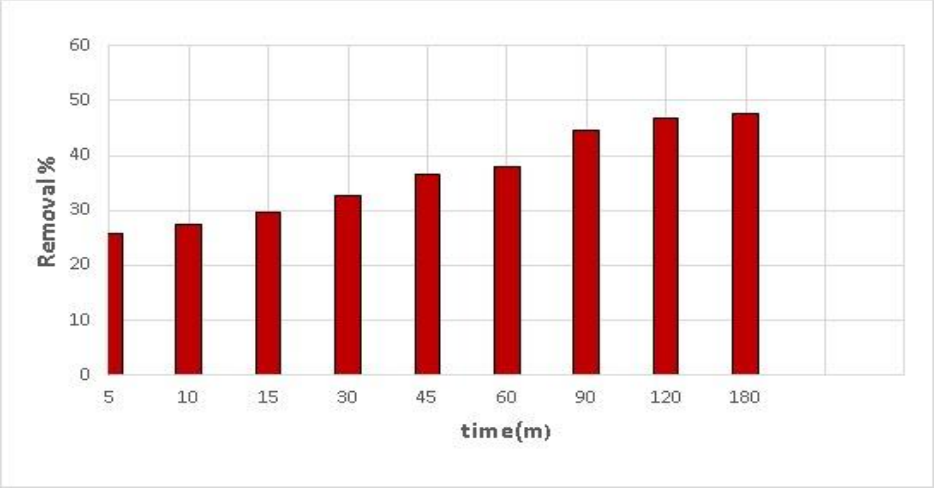

Figure 6: Percentage removal of moxifloxacin vs. time at 298 K and 0.3 g adsorbent

The γ-MNP was also used as a carrier for the MOX drug, which was loaded on the γ-MNP via impregnation method by stirring 15 mL of 30 mg. L^{-1} solutions of the drug with 0.3 g γ-MNP carrier for 24 h to achieve equilibrium. Subsequently, the drug-loaded mesoporous composite was obtained after being filtered and oven-dried for 12 h at 50°C [39]. The determinate quantity of MOX medicine loaded in the carrier was 1.75 mg of the drug per gram of carrier. A small quantity of drug-loaded carriers may be introduced into a substantial volume of release medium (PBS solution) using a dialysis bag to obtain the in vitro release profiles of pharmaceuticals [36, 40]. The drug-release behavior was investigated at 37 °C, pH = 7.4 and 5.4 (physiological condition), and the cumulative MOX release is shown in Figure 7.

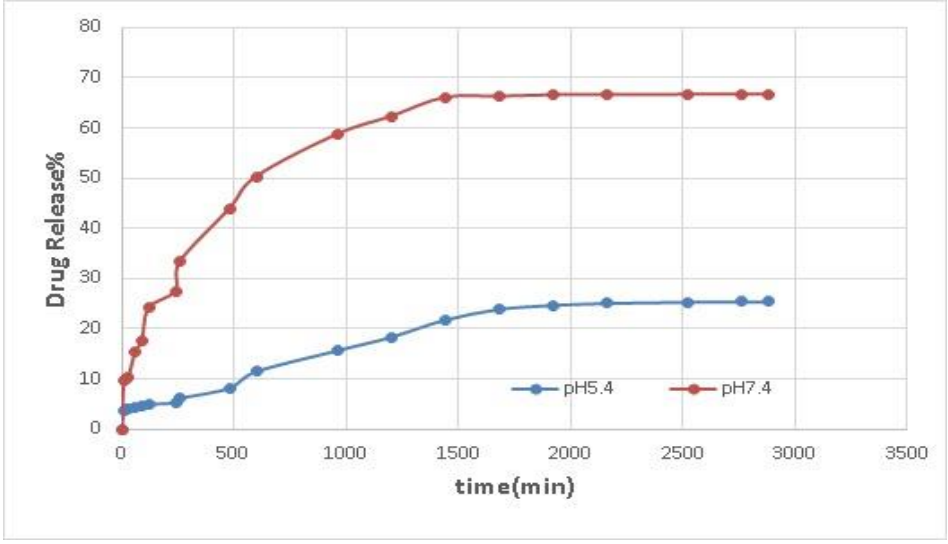

Figure 7: Release profile of MOX drug loaded γ-MNP at A) pH 7.4 and B) pH 5.4

Figure 7 shows that the MOX drug was approximately 66.05% released after 1440 min when the release occurred at pH 7.4, whereas at pH 5.4 the release decreased to 24.69% after 1920 min. The lower amount of MOX released at lower pH values has been attributed to the low solubility of the medicine in this condition [40]. The releasing profile of MOX with other carriers and our carrier with other drugs can be defined in references 39 and 40.

Conclusion

This study proposes a procedure that provides a very cost-efficient method for the successful production of mesoporous alumina nanoparticles using the extract of Zyziphus Spina Christi leaves as a natural surfactant and soft template in the sol-gel method. The mesoporous results were confirmed by SAXRD and N_2 adsorption–desorption analysis. Based on the particle size analysis, x-ray diffraction, SAXRD, AFM, SEM, and EDX analysis, the prepared alumina is in a crystalline form with γ- phase and has excellent texture properties for utilization as an adsorbent and carrier for MOX drug. The prepared γ-MNP utilized as an adsorbent to remove moxifloxacin (MOX) drug from the aqueous solution with approximately 47.64% of MOX was removed and as a carrier with approximately 66.05% released after 1440 min at pH 7.4, while at pH 5.4 the release decreased to 24.69% after 1920 min. Thus, this methodology can be used to effectively synthesize mesoporous alumina nanoparticles and can be used as a good adsorbent and carrier for MOX drugs.

Conflict of Interest

Conflicts of interest are not reported by the authors.

Acknowledgment

The authors would like to thank the College of Science, University of Baghdad, for presenting this work.

References

[1] K. Xia, S. Hou, Q. Niu, K. Suzuki, and P. Zhang, "Mechanochemical templated synthesis of mesoporous alumina-supported polyoxometalate catalysts toward selective oxidation of sulfides," *Royal Society of Chemistry Mechanochemistry*, vol. 2, no. 3, pp. 394-398, 2025.

[2] V. V. Vinogradov, A. V. Agafonov, A. V. Vinogradov, T. I. Gulyaeva, V. A. Drozdov, and V. A. Likholobov, "Sol–gel synthesis, characterization and catalytic activity of mesoporous γ-alumina prepared from boehmite sol by different methods," *Journal of Sol-Gel Science and Technology*, vol. 56, no. 3, pp. 333–339, 2010.

[3] S. Zarei, S. Sadighian, K. Rostamizadeh, M. Khalkhali, "Theragnostic Magnetic Core-Shell Nanoparticle as Versatile Nanoplatform for Magnetic Resonance Imaging and Drug Delivery", *Biointerface Research in Applied Chemistry*, vol. 11, no. 5, pp. 13276 – 13289, 2021. https://doi.org/10.33263/BRIAC115.1327613289 .

[4] M. Pourmadadi et al., "Porous alumina as potential nanostructures for drug delivery applications, synthesis and characteristics," *Journal of Drug Delivery Science and Technology*, vol. 77, no. 103877, p. 103877, 2022.

[5] C. B. Reid, J. S. Forrester, H. J. Goodshaw, E. H. Kisi, and G. J. Suaning, "A study in the mechanical milling of alumina powder," *Ceramics International*, vol. 34, no. 6, pp. 1551–1556, 2008.

[6] K. Yatsui, T. Yukawa, C. Grigoriu, M. Hirai, and W. Jiang, "Synthesis of ultrafine γ-Al2O3 powders by pulsed laser ablation," *Journal of Nanoparticle Research*, vol. 2, no. 1, pp. 75–83, 2000.

[7] F. Mirjalili, M. Hasmaliza, and L. C. Abdullah, "Size-controlled synthesis of nano α-alumina particles through the sol–gel method," *Ceramics International*, vol. 36, no. 4, pp. 1253–1257, 2010.

[8] R. Kavitha and V. Jayaram, "Deposition and characterization of alumina films produced by combustion flame pyrolysis," *Surface and Coatings Technology*, vol. 201, no. 6, pp. 2491–2499, 2006.

[9] L. Qu, C. He, Y. Yang, Y. He, and Z. Liu, "Hydrothermal synthesis of alumina nanotubes templated by anionic surfactant," *Materials Letters*, vol. 59, no. 29–30, pp. 4034–4037, (2005).

[10] S. Ghosh and M. K. Naskar, "Synthesis of mesoporous γ-alumina nanorods using a double surfactant system by reverse microemulsion process," *Royal Society of Chemistry Advances*, vol. 3, no. 13, p. 4207, 2013.

[11] Z. Wu, Q. Li, D. Feng, P. A. Webley, and D. Zhao, "Ordered mesoporous crystalline γ-Al2O3 with variable architecture and porosity from a single hard template," *Journal of the American Chemical Society*, vol. 132, no. 34, pp. 12042–12050, 2010.

[12] W. Wu, M. Zhu, and D. Zhang, "The role of solvent preparation in soft template assisted synthesis of mesoporous alumina," *Microporous and Mesoporous Materials*, vol. 260, pp. 9–16, 2018.

[13] H. Li, L. Wang, Y. Wei, W. Yan, and J. Feng, "Preparation of templated materials and their application to typical pollutants in wastewater: A review," *Frontiers in Chemistry*, vol. 10, p. 882876, 2022.

[14] D. Liu, Y.-Y. Hu, Y.-Y. Hu, C. Zeng, and D.-Y. Qu, "Soft-Templated Ordered Mesoporous CarbonMaterials: Synthesis, Structural Modification and Functionalization," *Acta Physico-Chimica Sinica*, vol. 32, no. 12, pp. 2826–2840, 2016.

[15] J. Zhao et al., "Microwave solvothermal fabrication of Zirconia hollow microspheres with different morphologies using pollen templates and their dye adsorption removal," *Industrial & Engineering Chemistry Research*, vol. 57, no. 1, pp. 231–241, 2018.

[16] M. A. Azeez, I. H. Ali, and S. H. Kareem, "Study of Micellar Behavior of a Tween 80 Surfactant in Aqueous Media Containing Diphenhydramine Hydrochloride," *Iraqi Journal of Science*, vol. 63, no. 8, pp. 3276–3282, 2022. DOI: 10.24996/ijs.2022.63.8.3.

[17] Y. Xie, D. Kocaefe, C. Chen, and Y. Kocaefe, "Review of research on template methods in preparation of nanomaterials," *Journal of Nanomaterials*, vol. 2016, pp. 1–10, 2016.

[18] J. Čejka, "Organized mesoporous alumina: synthesis, structure and potential in catalysis," *Applied Catalysis A: General*, vol. 254, no. 2, pp. 327–338, 2003.

[19] M. Sepehrian, F. Yazdi, and M. Anbia, "Extraction and green template-free synthesis of high-value mesoporous γ-Al2O3 and SiO2 powders from coal gangue," *Powder Technology*, vol. 444, no. 120023, p. 120023, 2024.

[20] G. S. Hassan and A. H. Abbar, "Electrocoagulation process for cobalt removal from industrial wastewater: Optimization and kinetic study," *South African Journal of Chemical Engineering*, vol. 53, pp. 233–241, 2025.

[21] I. Saptiama, F. Rindiyantono, A. Aries, Y. V. Kaneti, and M. Iqbal, "Synthesis and characterization of ordered and disordered mesoporous alumina as high-performance molybdenum-99 adsorbents," *Atom Indonesia*, vol. 47, no. 1, p. 45, 2021.

[22] W. K. Mahdi, A. O. Flayyih, and F. H. Musa, "Green synthesis, characterization, and applications of aluminum oxide nanoparticles using aqueous extract of clove," *Jurnal Kimia Valensi*, vol. 10, no. 2, pp. 277–289, 2024.

[23] I. L. Ikhioya and A. C. Nkele, "Green synthesis and characterization of aluminum oxide nanoparticle using neem leaf extract (Azadirachta Indica)," *Hybrid Advances*, vol. 5, no. 100141, pp. 100141, 2024.

[24] M. Kjellim and I. Johansson, *Surfactants from Renewable Resources*. John Wiley and Sons, Ltd, 2010.

[25] M. A. Ahmadi and S. R. Shadizadeh, "Adsorption of novel nonionic surfactant and particle mixture in carbonates: enhanced oil recovery implications," *Energy & Fuels*, vol. 26, pp. 4655–4663, 2012.

[26] M. A. Ahmadi and S. R. Shadizadeh, "Spotlight on the new natural surfactant flooding in carbonate rock samples in low salinity condition," *Scientific Reports*, vol. 8, no. 1, pp. 10985, 2018.

[27] A. A. Diyarov, N. Q. Mukhamadiev, M. Sayitkulov Sh, and J. R. Uzokov, "Synthesis of mesoporous sorbents on the basis of Al2O3 and their textural characteristics," *Central Asian Journal of Medical and Natural Science*, vol. 3, no. 3, pp. 511–518, 2022.

[28] K. M. Parida, A. C. Pradhan, J. Das, and N. Sahu, "Synthesis and characterization of nano-sized porous gamma-alumina by control precipitation method," *Materials Chemistry and Physics*, vol. 113, no. 1, pp. 244–248, 2009.

[29] A. K. Saleh, A. S. Shaban, M. A. Diab, D. Debarnot, and A. S. Elzaref, "Green synthesis and characterization of aluminum oxide nanoparticles using Phoenix dactylifera seed extract along with antimicrobial activity, phytotoxicity, and cytological effects on Vicia faba seeds," *Biomass Conversion and Biorefinery*, vol. 14, no. 24, pp. 31859–31875, 2024.

[30] Banerjee S, Gautam RK, Jaiswal A, M. Chandra Chattopadhyaya and Y. Chandra Sharma, "Rapid scavenging of methylene blue dye from a liquid phase by adsorption on alumina nanoparticles," *Royal Society of Chemistry Advances*, vol. 5, no. 19, pp. 14425–14440, 2015.

[31] T. Sun, Q. Zhuo, Y. Chen, and Z. Wu, "Synthesis of boehmite and its effect on flame retardancy of epoxy resin," *High Performance Polymers*, vol. 27, no. 1, pp. 100–104, 2015.

[32] X. Krokidis, P. Raybaud, A.-E. Gobichon, B. Rebours, P. Euzen, and H. Toulhoat, "Theoretical study of the dehydration process of boehmite to γ-alumina," *Journal of Physical Chemistry B*, vol. 105, no. 22, pp. 5121–5130, 2001. https://doi.org/10.1016/j.physchem.b .

[33] M. E. M. Babiker, "Eco-environmentally friendly green synthesis and characterization of aluminum oxide nanoparticles using leaf extract of Mentha pulegium," *International Journal of Chemistry and Biochemical Sciences*, vol. 25, no. 19, pp. 958-965, 2024.

[34] S. Mahdavi, A. Asghari-Alamdari, and M. Zolola-Meibodi, "Effect of alumina particle size on characteristics, corrosion, and tribological behavior of Co/Al2O3 composite coatings," *Ceramics International*, vol. 46, no. 4, pp. 5351–5359, 2020.

[35] M. Thommes, K. Kaneko, A. V. Neimark, J. P. Olivier, F. Rodriguez-Reinoso, J. Rouquerol and K. S. W. Sing, "Physisorption of gases, with special reference to the evaluation of surface area and pore size distribution (IUPAC Technical Report)," *Pure and Applied Chemistry*, vol. 87, no. 9–10, pp. 1051–1069, 2015.

[36] M. A. Sachit and S. H. Kareem, "Isotherms and thermodynamic parameters of metoprolol drug adsorption on the Prepared Mesoporous Silica," *Baghdad Science Journal*, vol. 21, no. 3, pp. 1029-1036, 2023. https://dx.doi.org/10.21123/bsj.2023.2288 .

[37] S. Banerjee, R. K. Gautam, A. Jaiswal, M. Chandra Chattopadhyaya, and Y. Chandra Sharma, "Rapid scavenging of methylene blue dye from a liquid phase by adsorption on alumina nanoparticles," *Royal Society of Chemistry Advances*, vol. 5, no. 19, pp. 14425–14440, 2015.

[38] D. Berger, G. Traistaru, and C. Matei, "Influence of different templates on the morphology of mesoporous aluminas," *Open Chemistry*, vol. 10, no. 5, pp. 1688–1695, 2012.

[39] N. M. Soliman, F. Shakeel, N. Haq, F. K. Alanazi, S. Alshehri, M. Bayomi, A.S.M. Alenazi, I.A. Alsarra, "Development and optimization of ciprofloxacin HCl-loaded chitosan nanoparticles using Box-Behnken experimental design," *Molecules*, vol. 27, no. 14, pp. 4468, 2022.

[40] L. É. Uhljar, S. Y. Kan, N. Radacsi, V. Koutsos, P. Szabó-Révész, and R. Ambrus, "In vitro drug release, permeability, and structural test of ciprofloxacin-loaded nanofibers," *Pharmaceutics*, vol. 13, no. 4, p. 556, 2021.